Radiobiological Models

Past, Present and Future Directions

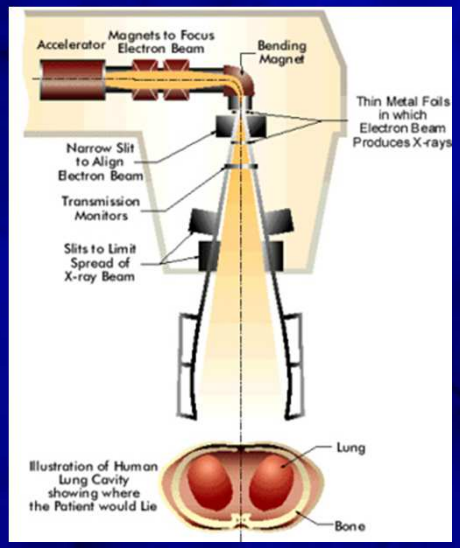

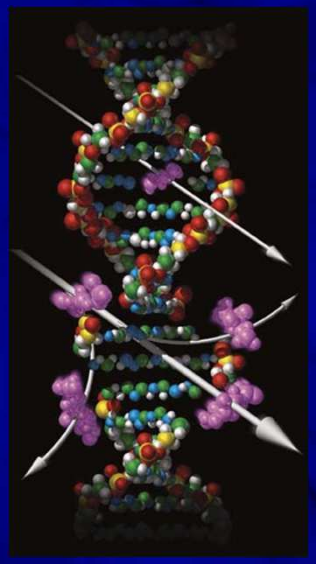

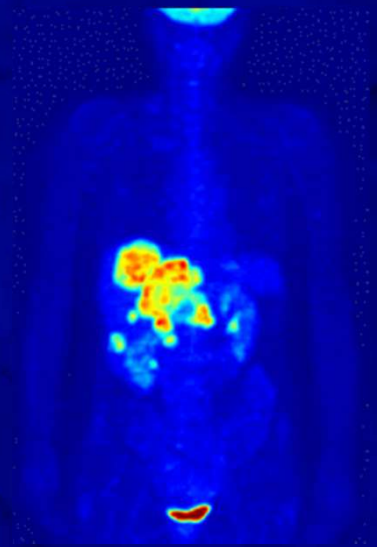

Dr. G.V. Giri

Dr. Sanjay S. Supe

Kidwai Memorial Institute of Oncology

Bangalore

14.6 CELL SURVIVAL CURVES

Typical survival curves for cells irradiated by densely ionizing radiation (high LET) and sparsely ionizing radiation (low LET).

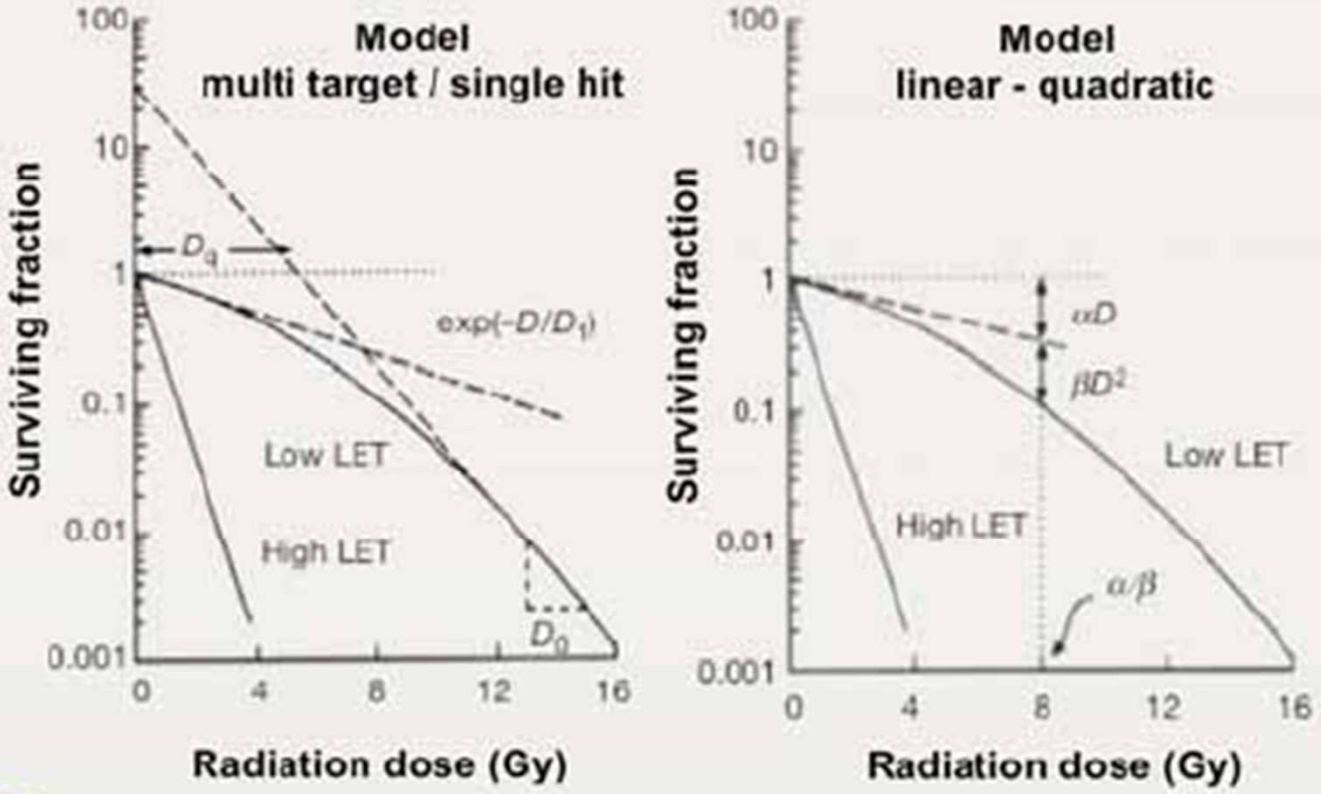

14.7 DOSE RESPONSE CURVES

- A plot of a biological effect observed (e.g., tumour induction or tissue response) against the dose given is called a dose response curve.
- Dose response may refer to:
  - Clonogenic end points, i.e., cell survival.
  - Functional end points.
- Generally, as the dose increases so does the effect.

14.7 DOSE RESPONSE CURVES

- Three types of dose response relationships are known:
  - Linear
  - Linear-quadratic
  - Sigmoid
- Dose response curves may or may not have a threshold dose.
- A threshold dose is the largest dose for a particular effect studied below which no such effect will be observed.

14.7 DOSE RESPONSE CURVES

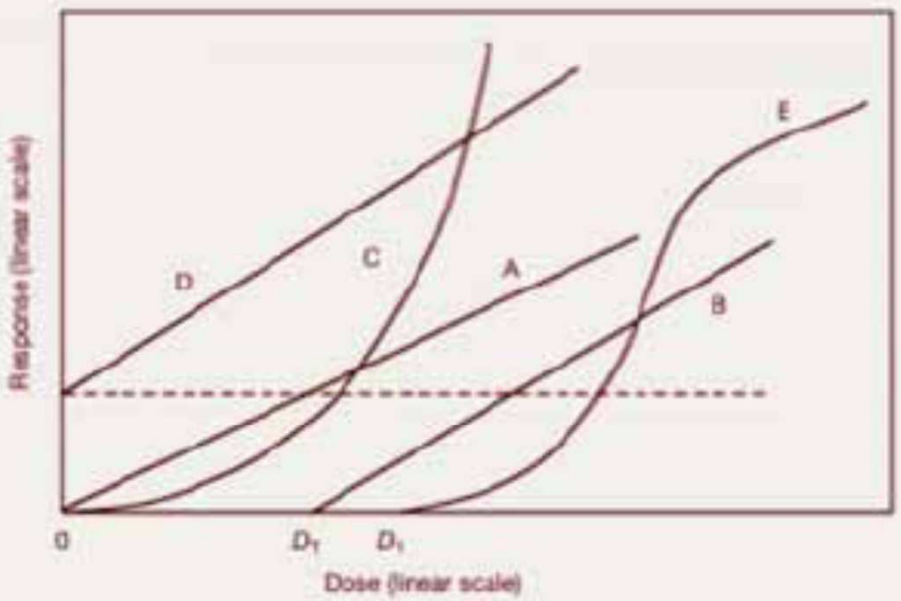

Dose response curves

(A) Linear relationship with no threshold

(B) Linear relationship with threshold

(C) Linear-quadratic relationship with no threshold (stochastic effects such as carcinogenesis)

(D) Linear relationship with no threshold and the area under the dashed line representing the natural incidence of the effect.

(E) Sigmoid relationship with threshold D1, as is common for deterministic effects in tissues.

14.7 DOSE RESPONSE CURVES

- The response of tissues or organs to radiation varies markedly, depending on two factors:
  - Inherent sensitivity of the individual cells
  - Kinetics of the population
- With regard to response time two types of tissue are known:
  - Early responding (skin, mucosa, intestinal epithelium).
  - Late responding (spinal cord).

14.7 DOSE RESPONSE CURVES

Properties of cell survival curves:

- For late responding tissues the survival curves are more curved than those for early responding tissues.
- For early effects the ratio α/β is large; for late effects it is small.
- For early effects α dominates at low doses.
- For late effects β has an influence at doses lower than for early responding tissues.
- The α and β components of mammalian cell killing are equal at the following doses:
  - $\alpha/\beta \approx 10$ Gy for early responding tissues
  - $\alpha/\beta \approx 3$ Gy for late responding tissues

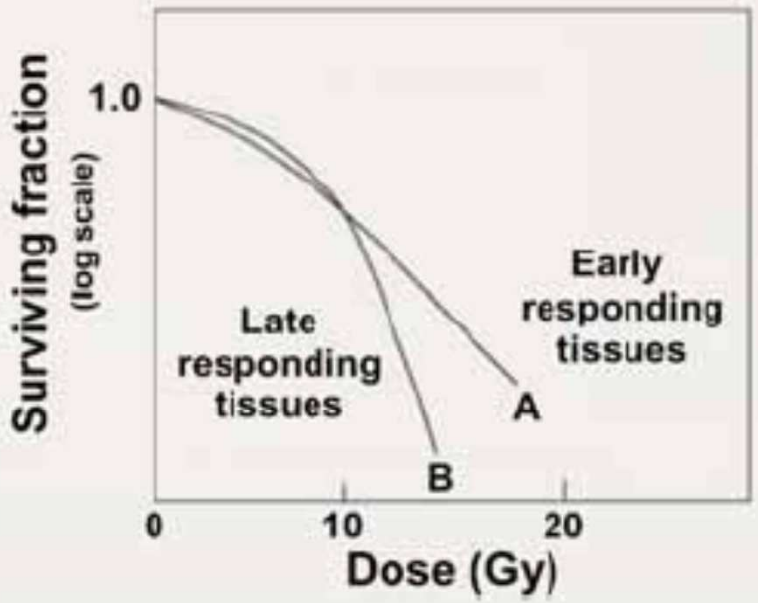

14.8 TYPE OF RADIATION DAMAGE

- The effects of radiation on tissue as a function of dose are measured with assays and the measured results are presented in the form of:
  - Cell survival curves
  - Dose response curves.

14.8 TYPE OF RADIATION DAMAGE

- Three categories of tissue assay are in use:
  - Clonogenic assays measure the reproductive integrity of the clonogenic stem cells in tissue and the measurements result in cell survival curves.
  - Functional assays measure functional end points for various tissues and produce dose response curves.
  - Lethality assays quantify the number of animal deaths after irradiation of the whole animal or of a specific organ with a given dose. The experiments are usually presented with parameter LD_{50}.

14.9 NORMAL AND TUMOUR CELLS: THERAPEUTIC RATIO

- Cancer is characterized by a disorderly proliferation of cells that can invade adjacent tissues and spread via the lymphatic system or blood vessels to other parts of the body.
- The aim of radiotherapy is to deliver enough radiation to the tumour to destroy it without irradiating normal tissue to a dose that will lead to serious complications (morbidity).

14.9 NORMAL AND TUMOUR CELLS: THERAPEUTIC RATIO

- The principle of radiotherapy is usually illustrated by plotting two sigmoid curves
  - For tumour control probability (TCP)
  - For normal tissue complication probability (NTCP)

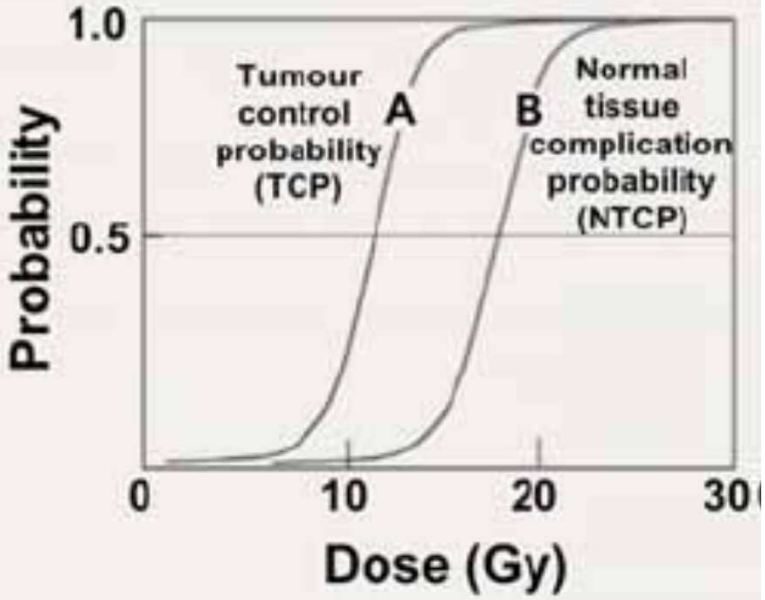

14.9 NORMAL AND TUMOUR CELLS: THERAPEUTIC RATIO

- The optimum choice of radiation dose delivery technique in the treatment of a given tumour is such that it maximizes the TCP and simultaneously minimizes the NTCP.
- For a typical good radiotherapy treatment:
  - TCP $\geq$ 0.5
  - NTCP $\geq$ 0.05

14.9 NORMAL AND TUMOUR CELLS: THERAPEUTIC RATIO

- The concept of the therapeutic ratio is often used to represent the optimal radiotherapy treatment.
- Therapeutic ratio generally refers to the ratio of the TCP and NTCP at a specified level of response (usually 0.05) for normal tissue.

14.9 NORMAL AND TUMOUR CELLS: THERAPEUTIC RATIO

- The further the NTCP curve is to the right of the TCP curve:
  - the easier it is to achieve the radiotherapeutic goal
  - the larger is the therapeutic ratio
  - the less likely are treatment complications

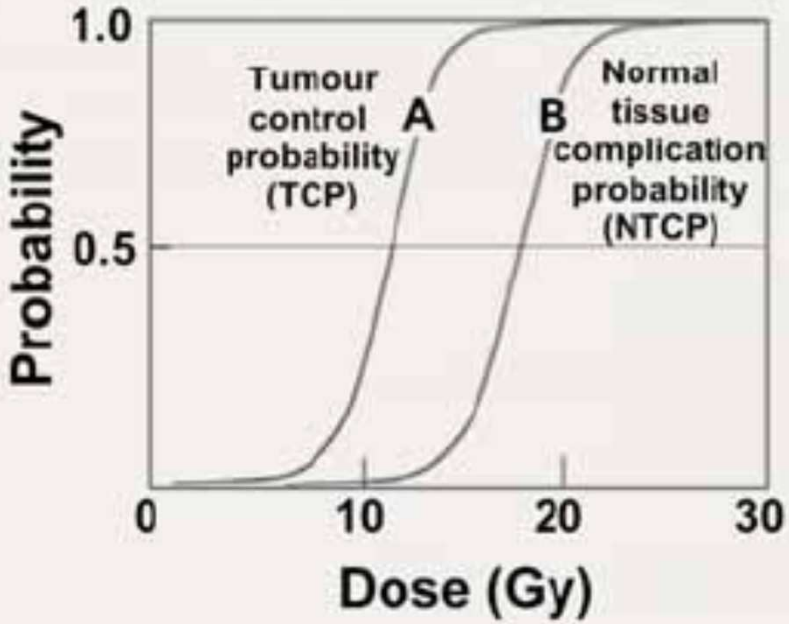

14.9 NORMAL AND TUMOUR CELLS: THERAPEUTIC RATIO

- The TCP curve for regional control of certain tumours never reaches a value of 1.0 as a result of microscopic or metastatic spread of the disease beyond the primary tumour site.
- It is imperative that the doses to normal tissues be kept lower than the doses to tumours in order to:
  - Minimize treatment complications.
  - Optimize treatment outcomes.

14.9 NORMAL AND TUMOUR CELLS: THERAPEUTIC RATIO

- In modern radiotherapy these objectives are met through:
  - Sophisticated 3-D treatment planning (forward as well as inverse)
  - Accurate target localization
  - Sophisticated dose delivery (conformal, intensity modulated, image-guided).
- In the early days of radiotherapy it was assumed that normal cells were less sensitive to single doses of radiation than tumour cells.

14.9 NORMAL AND TUMOUR CELLS: THERAPEUTIC RATIO

- Currently, it is accepted that both malignant cells and those normal cells responsible for early reactions exhibit similar values for $D_0 \approx 1.3$ Gy, with $\alpha/\beta \approx 10$ Gy.
- It is for late reactions in general that the shoulder on the target cell survival curve is effectively greater than it is for target cells in tumours or early responding tissues with $\alpha/\beta \approx 3$, thus providing a differential that is exploited in hyper-fractionation protocols to spare (reduce) late reactions using small dose fractions.

Fowler (1988)

The most important point about any biological models is that you should not believe in them too much. Their proper use is as rough guidelines and as prompts for further thoughts.

RT Process

Conventional RT Paradigm

Treatment Parameters

Dose Calc

Dose Distribution

Dose delivery with Uniform Radiation Intensity

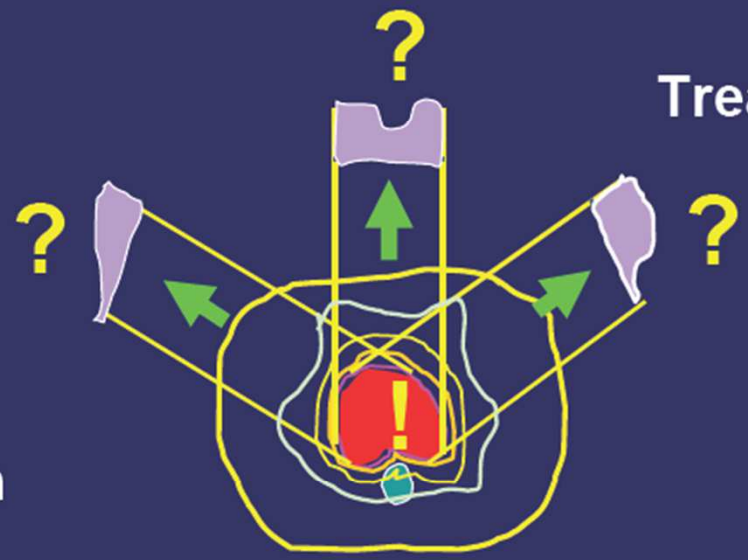

IMRT Paradigm

Dose delivery with Non-uniform Radiation Intensity

Treatment Parameters

Treatment Goals (Objective Function)

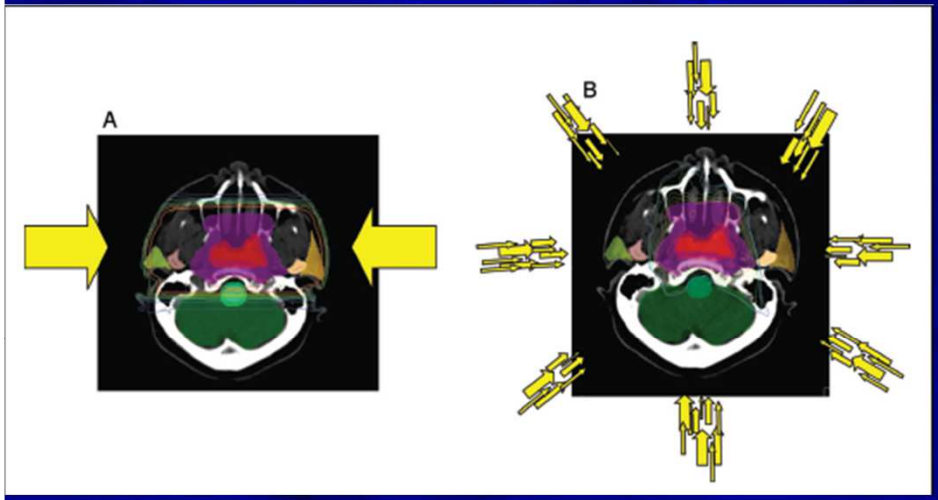

Complex & Unconventional Dose Distributions

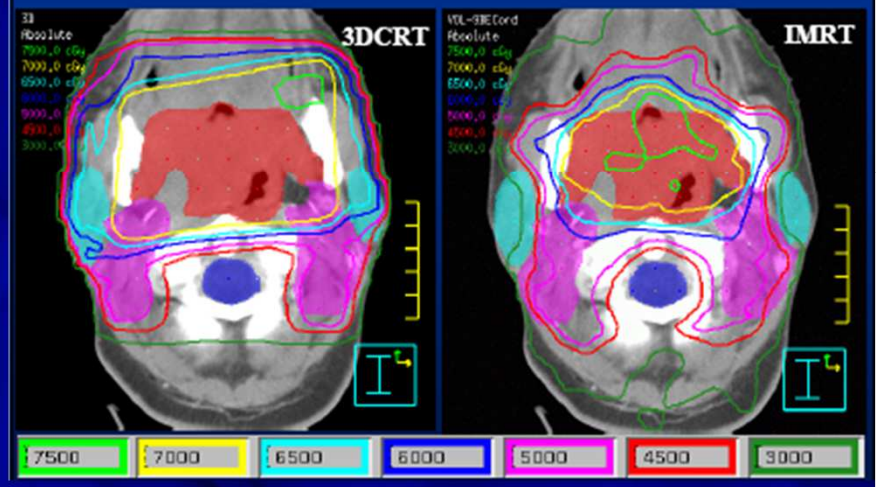

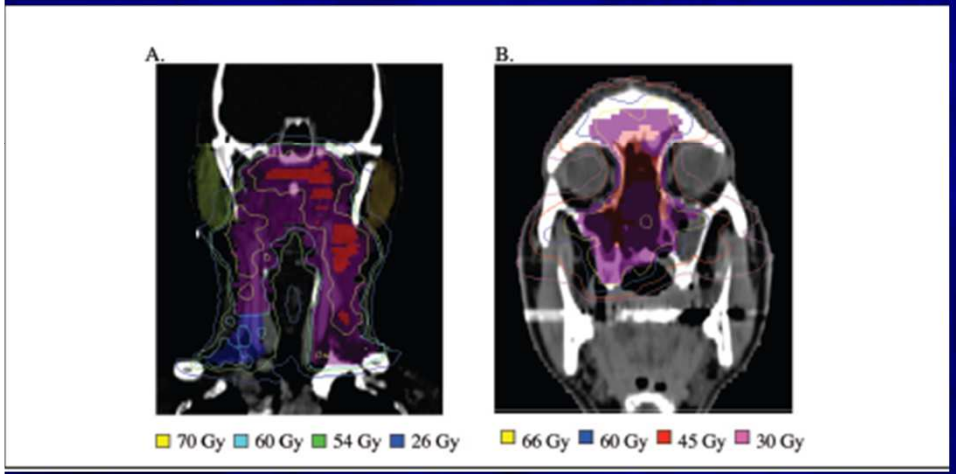

‘Chain’ of IMRT Process

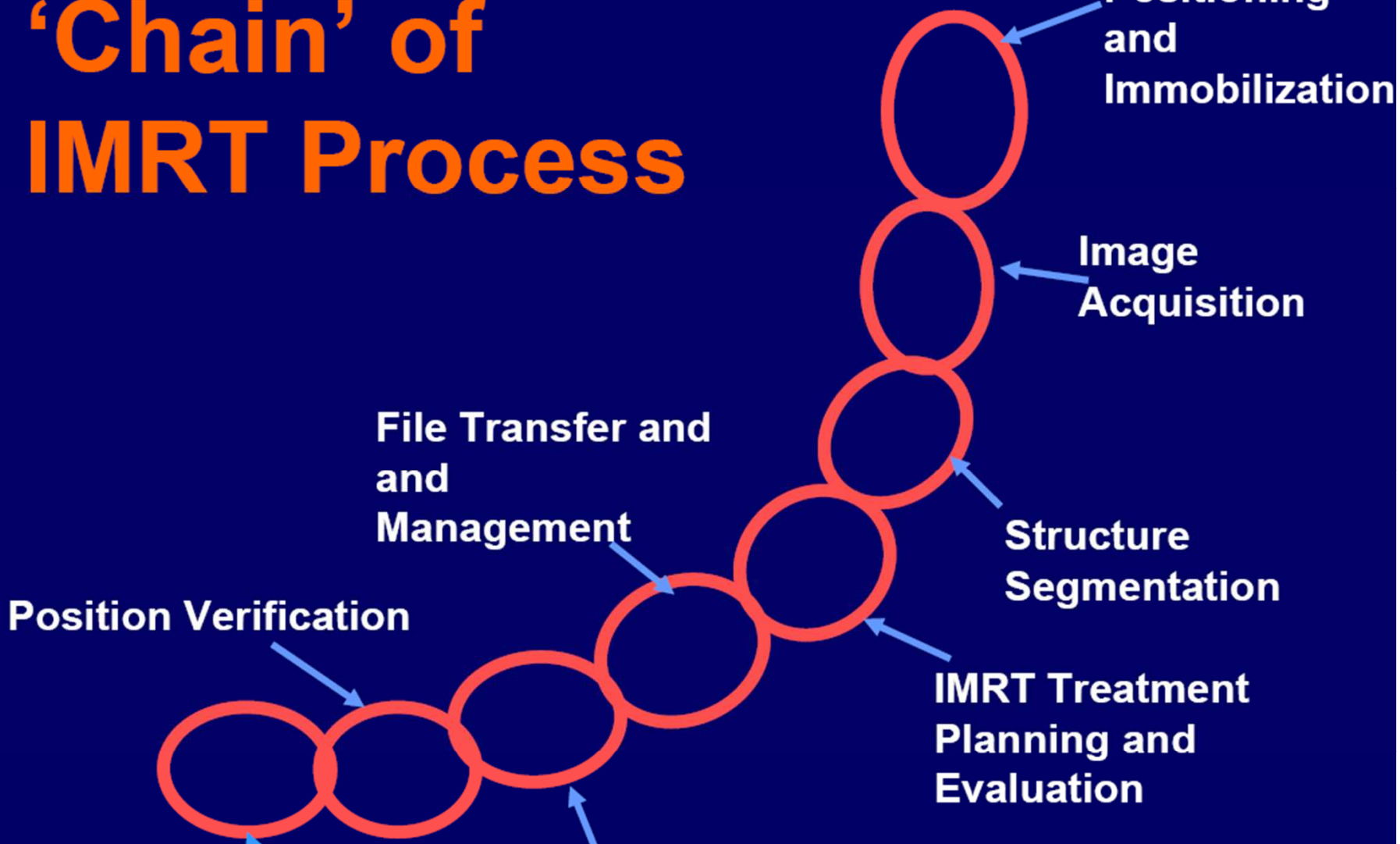

Adapted from an illustration presented by Webb, 1996

R’s of Radiobiology

- ✓ Repair
- ✓ Repopulation
- ✓ Reoxygenation
- ✓ Redistribution
- ✓ Regression
- ✓ Recruitment
- ✓ Reseeding
- ✓ Radiosensitivity

Use of bioeffect models in Radiotherapy

- ✓ Retrospective analysis of clinical data
- ✓ Design of treatment schemes
- ✓ Modification of treatment schemes
- ✓ Determination of TCP and NTCP
- ✓ Prospective analysis of clinical data
- ✓ Arriving at tolerance biological dose values

$$\mathrm{NSD} = D\, N^{-0.24}\, T^{-0.11}$$

$$\mathrm{CRE} = d\, n^{0.65}\, x^{-0.11}$$

$$\mathrm{CRE_c} = 0.53\, D\, T^{-0.29} = 0.53\, R\, T^{-0.71}$$

$$\mathrm{TDF} = d^{1.538}\, n\, x^{-0.169}\, 10^{-3}$$

$$\mathrm{TDF_c} = 4.76\, R^{1.35}\, T\, 10^{-3}$$

What about the tumour ?

$$\mathrm{TSD} = d\, n^{0.76}\, x^{-0.06}$$

$$\mathrm{TDF_t} = d^{1.316}\, n\, x^{-0.079}\, (5 \cdot 10^{-3})$$

Fowler (1988)

NSD, CRE, TDF be consigned to the historical museum. The place occupied by them in the museum must be an honoured one.

Orton (1988)

But some are useful. Provided the user realizes that all the models provide approximate representations of the highly complex series of biological events which occur during the course of radiotherapy, then the models are really useful.

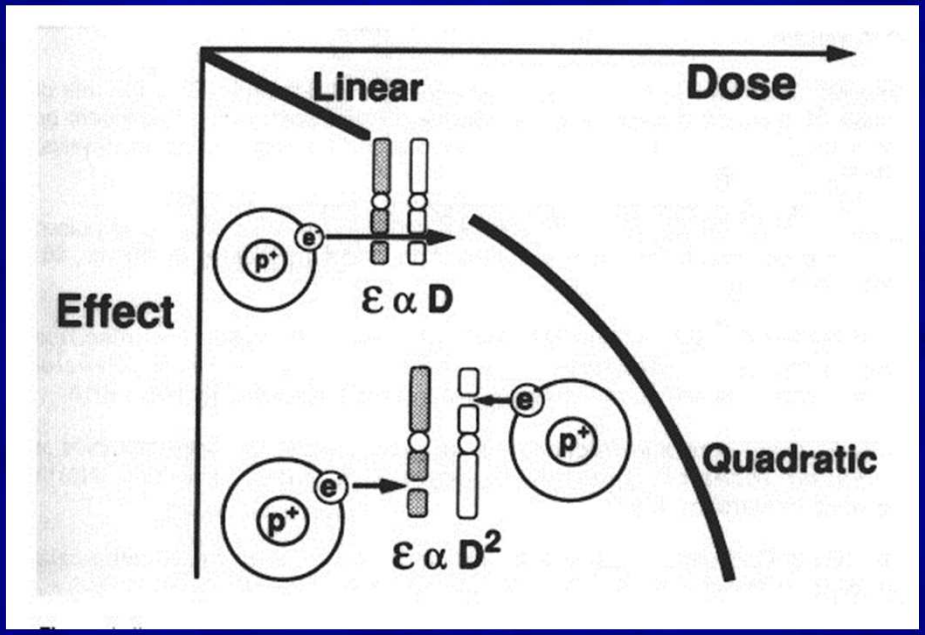

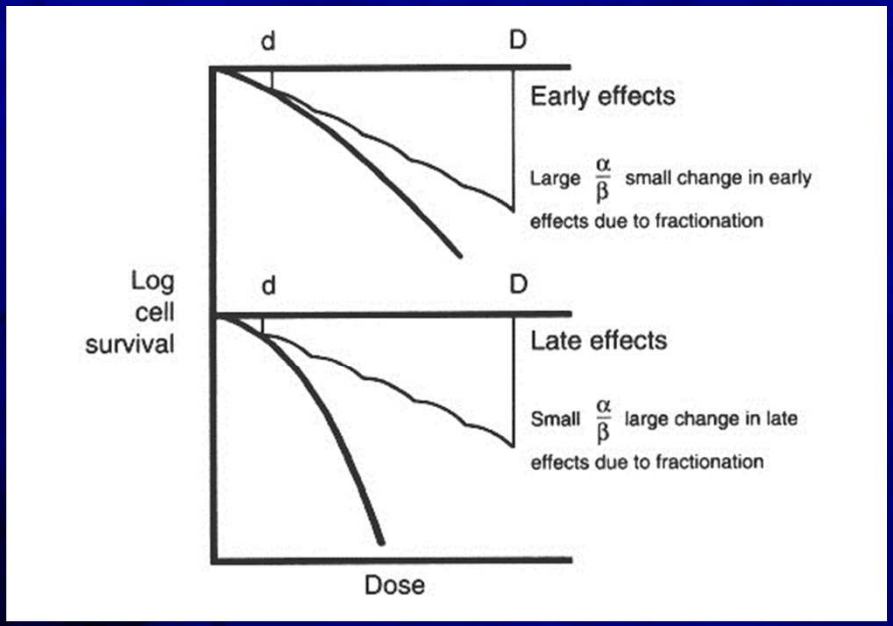

Basic Equations of the L-Q Model

The L-Q model was originally proposed for fractionated radiotherapy by Fowler & Stern (1960,1963) and has been refined and expanded by Barendsen (1982) and Dale (1985). The bioeffect dose for the L-Q model is the extrapolated response dose (ERD), and the basic ERD equations for HDR (teletherapy & HDR brachytherapy) and for LDR continuous brachytherapy are as follows.

HDR: $$ERD\text{-}Nd\left(1+\frac{d}{\alpha/\beta}\right) \quad [1]$$

LDR: $$ERD\text{-}NRt\left[1+\frac{2R}{\mu(\alpha/\beta)}\left(1-\frac{1-e^{-\mu t}}{\mu t}\right)\right] \quad [2]$$

where:

N = number of fractions (for HDR or LDR);

d = dose/fraction (for HDR) in Gy;

R = dose rate (for LDR) in Gy/hour;

t = time for each fraction (for LDR) in hours;

and α/β (in Gy) and μ (in h^{-1}) are tissue-specific parameters.

If the overall treatment time is T days, then the tumour BED may be corrected for concurrent tumour repopulation via:

$$\mathrm{BED} = Nd\left[1 + \frac{d}{(\alpha/\beta)}\right] - KT \qquad \text{(A2)}$$

where K is the dose equivalent of daily repopulation, defined in terms of intrinsic radiosensitivity (α) and potential doubling time (T_{pot}) as:

$$K = \frac{0.693}{\alpha T_{pot}} \qquad \text{(A3)}$$

Dale (1994)

The suggested form of the FOM, which utilizes the ratio $\mathrm{BED}_{new}/\mathrm{BED}_{ref}$ for both the tumour and critical tissue, is as follows:

$$\mathrm{FOM} = [10 \times (\mathrm{BED}_{new}/\mathrm{BED}_{ref})_{tum}{}^{Z}]^{X} \qquad (6)$$

where:

$$Z = 2.5 \text{ when } (\mathrm{BED}_{new}/\mathrm{BED}_{ref})_{tum} \geqslant 1.0$$

$$Z = 8 \text{ when } (\mathrm{BED}_{new}/\mathrm{BED}_{ref})_{tum} < 1.0$$

and:

$$X = [(\mathrm{BED}_{ref}/\mathrm{BED}_{new})_{crit}{}^{Y}]$$

with:

$$Y = 2 \text{ when } (\mathrm{BED}_{new}/\mathrm{BED}_{ref})_{crit} \geqslant 1.05$$

$$Y = 1 \text{ when } (\mathrm{BED}_{new}/\mathrm{BED}_{ref})_{crit} < 1.05$$

Table 2.1 **Typical range of values observed for LQ model parameters and some suggested "generic" values (in paranthesis) that are frequently employed when more definitive values are not available**

Tissue	α/β (Gy)	μ (hr^{-1})	K (Gy/day)	T_0 (days)
Late responding	1 – 5 (2.5)	0.3 – 1 (0.46)	0 – 0.1 (0)	0 – 20 (0)
Early responding	1 – 15 (10)	0.3 – 2.0 (0.46 or 1.4)	0.2 – 0.4 (0.3)	0 – 30 (0)
Tumour	5 – 30 (10 or 20)	0.3 – 2.0 (0.46 or 1.4)	0 – 1 (0.72)	0 – 30 (14 or 28)

Carcinoma of the cervix

Tissue	α/β (Gy)	μ (hr^{-1})	K (Gy/day)	T_0 (day)
Tumour Point A	10.0	0.69	0.5	28
Rectum	3.87	0.46	0	0
Bladder	4.00	0.46	0	0

Head and neck cancer

Tissue	α/β (Gy)	μ (hr^{-1})	K (Gy/day)	T_0 (day)
Tumour	13.4	0.69	0.76	28
Early resp	11.2	1.40	0.5	28
Late resp	4.3	0.46	0	0

ELSEVIER

Medical Dosimetry, Vol. 25, No. 2, pp. 71–76, 2000

0958-3947/00/$–see front matter

PII: S0958-3947(00)00031-5

BIOPLAN: SOFTWARE FOR THE BIOLOGICAL EVALUATION OF RADIOTHERAPY TREATMENT PLANS

B. SANCHEZ-NIETO and A. E. NAHUM

Joint Department of Physics, Royal Marsden NHS Trust and the Institute of Cancer Research, Sutton, Surrey, UK

(*Accepted* 22 *February* 2000)

Abstract—Distributions of absorbed dose do not provide information on the biological response of tissues (either tumor or organs at risk [OAR]) to irradiation. BIOPLAN (BIOlogical evaluation of PLANs) has been conceived and developed as a PC-based user-friendly software that allows the user to evaluate a treatment plan from the (more objective) point of view of the biological response of the irradiated tissues, and at the same time, provides flexibility in the use of models and parameters. It requires information on dose-volume histograms (DVHs) and can accept a number of different formats (including DVH files from commercial treatment planning systems). BIOPLAN provides a variety of tools, such as tumor control probability (TCP) calculations (using the Poisson model), normal tissue complication probability (NTCP) calculations (using either the Lyman-Kutcher-Burman or the relative seriality models), the ΔTCP method, DVH subtraction, plots of NTCP/TCP as a function of prescription dose, tumor and OAR dose statistics, equivalent uniform dose (EUD), individualized dose prescription, and parametric sensitivity analysis of the TCP/NTCP models employed. © 2000 American Association of Medical Dosimetrists.

Key Words: Biological evaluation, TCP, NTCP, DVH, Radiotherapy.

$$NTCP = 1/\sqrt{2\pi}\int_{-\infty}^{t}\exp(-x^2/2)\,dx$$

$$t = \frac{D - TD_{50}(v)}{m \cdot TD_{50}(v)}$$

$$TD_{50}(v) = TD_{50}(1) \cdot v^{-n}$$

$$TCP = \sum_i g_i(\sigma_\alpha) \cdot TCP(\alpha_i, \beta_i)$$

$$TCP(\alpha_i, \beta_i) = \prod_j TCP(\alpha_i, \beta_i, D_j, v_j)$$

$$= \prod_j \exp\left[-p_c \cdot v_j \cdot \exp\left(-\alpha_i \cdot D_j \cdot \left(1 + \frac{d_j}{\alpha_i/\beta_i}\right) + \gamma \cdot (T - T_k)\right)\right]$$

$$g_i(\sigma_\alpha) \propto \left(\frac{1}{\sigma_\alpha \cdot \sqrt{2\pi}}\right) \cdot \exp\left[\frac{-(\alpha_i - \overline{\alpha})^2}{2 \cdot \sigma_\alpha^2}\right]$$

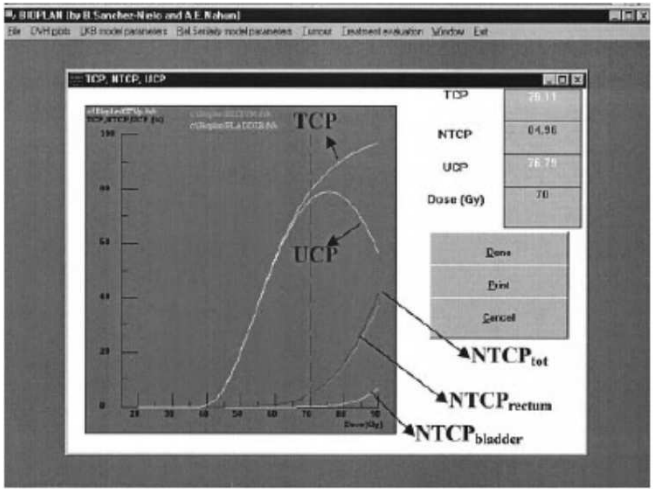

Fig. 1. BIOPLAN screen window showing the plot of TCP, NTCP, and UCP vs. prescription dose for a specific radiotherapy plan. A prostate treatment plan has been chosen as an example (DVH files for the prostate, GTV, bladder, and rectum were used). The LKB model has been used for the NTCP calculations. The different colors displayed in the computer screen identify each plot and make possible the link between curves and numbers displayed on the right. As this picture is shown in black and white, arrow lines pointing to each curve have been added to identify them.

Reporting and analyzing dose distributions: A concept of equivalent uniform dose

Andrzej Niemierko
Division of Radiation Biophysics, Department of Radiation Oncology, Massachusetts General Hospital, Boston, Massachusetts 02214, and Harvard Medical School, Boston, Massachusetts

(Received 21 August 1995; accepted for publication 30 September 1996)

Modern treatment planning systems for three-dimensional treatment planning provide three-dimensionally accurate dose distributions for each individual patient. These data open up new possibilities for more precise reporting and analysis of doses actually delivered to irradiated organs and volumes of interest. A new method of summarizing and reporting inhomogeneous dose distributions is reported here. The concept of equivalent uniform dose (EUD) assumes that any two dose distributions are equivalent if they cause the same radiobiological effect. In this paper the EUD concept for tumors is presented, for which the probability of local control is assumed to be determined by the expected number of surviving clonogens, according to Poisson statistics. The EUD can be calculated directly from the dose calculation points or, from the corresponding dose-volume distributions (histograms). The fraction of clonogens surviving a dose of 2 Gy (SF_2) is chosen to be the primary operational parameter characterizing radiosensitivity of clonogens. The application of the EUD concept is demonstrated on a clinical dataset. The causes of flattening of the observed dose-response curves become apparent since the EUD concept reveals the finer structure of the analyzed group of patients in respect to the irradiated volumes and doses actually received. Extensions of the basic EUD concept to include nonuniform density of clonogens, dose per fraction effects, repopulation of clonogens, and inhomogeneity of patient population are discussed and compared with the basic formula.
[S0094-2405(97)00501-4]

Key words: effective uniform dose, EUD, reporting dose, dose-volume distribution, DVH, three-dimensional treatment planning, biological modeling

A. The simplest models

$$\mathrm{EUD}(\mathrm{Gy}) = D_{\mathrm{ref}} \cdot \frac{\ln\left[\sum_{i=1}^{N} v_i \cdot (\mathrm{SF}_2)^{D_i/D_{\mathrm{ref}}}\right]}{\ln(\mathrm{SF}_2)}$$

or

$$\mathrm{EUD}(\mathrm{Gy}) = D_{\mathrm{ref}} \cdot \ln\left[\frac{1}{N}\sum_{i=1}^{N} (\mathrm{SF}_2)^{D_i/D_{\mathrm{ref}}}\right] \Big/ \ln(\mathrm{SF}_2).$$

B. Absolute volume effect

$$\mathrm{EUD}(V_{\mathrm{ref}}) = D_{\mathrm{ref}} \cdot \ln\left[(1/V_{\mathrm{ref}})\sum_{i=1}^{N} V_i \cdot (\mathrm{SF}_2)^{D_i/D_{\mathrm{ref}}}\right] \Big/ \ln(\mathrm{SF}_2),$$

C. Nonuniform spatial distribution of clonogens

$$\mathrm{EUD} = D_{\mathrm{ref}} \cdot \ln\left\{\frac{\left[\sum_{i=1}^{N} V_i \cdot \rho_i \cdot (\mathrm{SF}_2)^{D_i/D_{\mathrm{ref}}}\right]}{\sum_{i=1}^{N} V_i \cdot \rho_i}\right\} \Big/ \ln(\mathrm{SF}_2), \quad (10)$$

D. Dose-per-fraction effect

$$\mathrm{EUD} = \frac{N_f}{D_{\mathrm{ref}}} \cdot \left[-\frac{\alpha}{\beta} + \sqrt{\left(\frac{\alpha}{\beta}\right)^2 + 4 \cdot \frac{D_{\mathrm{ref}}}{N_f} \cdot \left(\frac{\alpha}{\beta} + D_{\mathrm{ref}}\right) \cdot \frac{\ln A}{\ln(\mathrm{SF}_2)}}\right]. \quad (13)$$

E. Proliferation effect

$$\mathrm{SF}(D) = 2^{[(T-T_k)/T_{\mathrm{pot}}]} \cdot (\mathrm{SF}_2)^{D/D_{\mathrm{ref}} \cdot \left(\frac{\alpha/\beta + D/N_f}{\alpha/\beta + D_{\mathrm{ref}}}\right)}.$$

F. Inhomogeneity of patient population

$$\mathrm{EUD} = \frac{1}{\sqrt{2 \cdot \pi} \cdot \sigma} \int_{-\infty}^{+\infty} \exp\left(-\frac{(S-\tilde{S})^2}{2 \cdot \sigma^2}\right) \cdot \mathrm{EUD}(S)\, dS, \quad (16)$$

Int. J. Radiation Oncology Biol. Phys., Vol. 53, No. 1, pp. 224–235, 2002
Copyright © 2002 Elsevier Science Inc.
Printed in the USA. All rights reserved
0360-3016/02/$–see front matter

PII S0360-3016(01)02585-8

PHYSICS CONTRIBUTION

OPTIMIZATION OF INTENSITY-MODULATED RADIOTHERAPY PLANS BASED ON THE EQUIVALENT UNIFORM DOSE

QIUWEN WU, PH.D.,* RADHE MOHAN, PH.D.,* ANDRZEJ NIEMIERKO, PH.D.,† AND RUPERT SCHMIDT-ULLRICH, M.D.*

*Department of Radiation Oncology, Medical College of Virginia, Virginia Commonwealth University and McGuire Veterans Affairs Hospital, Richmond, VA; †Department of Radiation Oncology, Massachusetts General Hospital and Harvard University, Boston, MA

Purpose: The equivalent uniform dose (EUD) for tumors is defined as the biologically equivalent dose that, if given uniformly, will lead to the same cell kill in the tumor volume as the actual nonuniform dose distribution. Recently, a new formulation of EUD was introduced that applies to normal tissues as well. EUD can be a useful end point in evaluating treatment plans with nonuniform dose distributions for three-dimensional conformal radiotherapy and intensity-modulated radiotherapy. In this study, we introduce an objective function based on the EUD and investigate the feasibility and usefulness of using it for intensity-modulated radiotherapy optimization.

Methods and Materials: We applied the EUD-based optimization to obtain intensity-modulated radiotherapy plans for prostate and head-and-neck cancer patients and compared them with the corresponding plans optimized with dose–volume-based criteria.

Results: We found that, for the same or better target coverage, EUD-based optimization is capable of improving the sparing of critical structures beyond the specified requirements. We also found that, in the absence of constraints on the maximal target dose, the target dose distributions are more inhomogeneous, with significant hot spots within the target volume. This is an obvious consequence of unrestricted maximization target cell kill and, although this may be considered beneficial for some cases, it is generally not desirable. To minimize the magnitude of hot spots, we applied dose inhomogeneity constraints to the target by treating it as a "virtual" normal structure as well. This led to much-improved target dose homogeneity, with a small, but expected, degradation in normal structure sparing. We also found that, in principle, the dose–volume objective function may be able to arrive at similar optimum dose distributions by using multiple dose–volume constraints for each anatomic structure and with considerably greater trial-and-error to adjust a large number of objective function parameters.

Conclusion: The general inference drawn from our investigation is that the EUD-based objective function has the advantage that it needs only a small number of parameters and allows exploration of a much larger universe of solutions, making it easier for the optimization system to balance competing requirements in search of a better solution. © 2002 Elsevier Science Inc.

Intensity-modulated radiotherapy, IMRT, Optimization, Biologic models, Equivalent uniform dose.

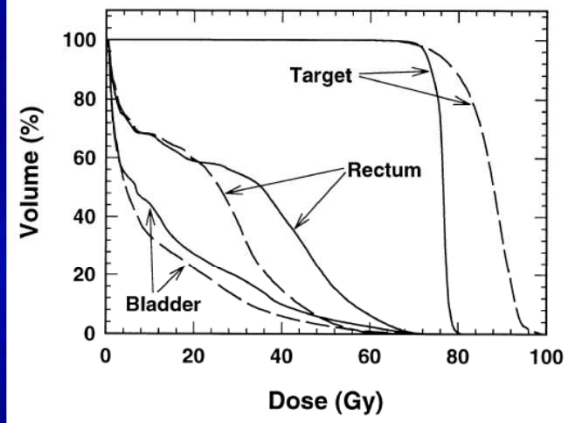

Fig. 5. Dose–volume histograms for the prostate plans of Fig. 4. Target, rectum, and bladder are shown. Solid lines indicate dose–volume-based criteria and dashed lines EUD-based criteria with no constraint on target dose inhomogeneity.

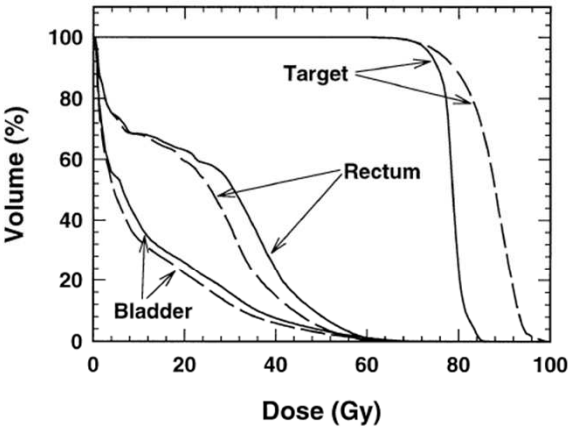

Fig. 7. Comparison of DVHs of prostate plans with EUD based-optimization and with (solid lines) and without (dashed lines) dose inhomogeneity constraints on the target.

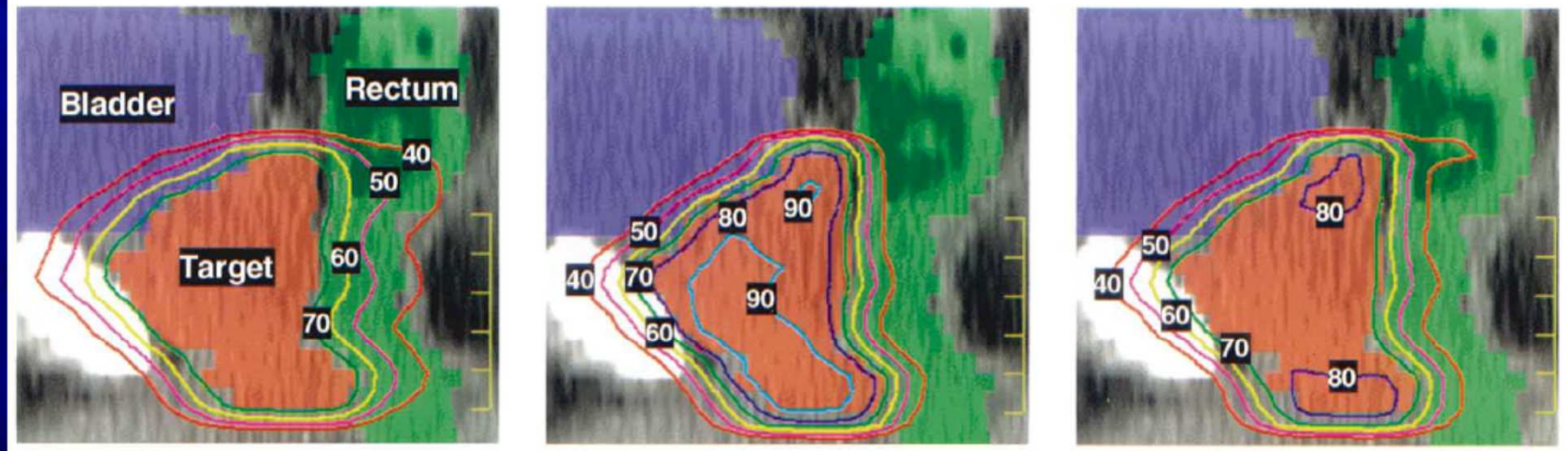

Fig. 4. Sagittal isodose distributions for prostate IMRT plans designed using (a) dose–volume-based criteria, (b) EUD-based criteria, and (c) EUD-based criteria with target inhomogeneity constraints.

A comparison of physically and radiobiologically based optimization for IMRT

Lois Jones[a)]
Department of Radiation Oncology, Liverpool Hospital, Australia

Peter Hoban
Department of Radiation Oncology, Prince of Wales Hospital, Australia

(Received 2 October 2001; accepted for publication 29 April 2002; published 20 June 2002)

Many optimization techniques for intensity modulated radiotherapy have now been developed. The majority of these techniques including all the commercial systems that are available are based on physical dose methods of assessment. Some techniques have also been based on radiobiological models. None of the radiobiological optimization techniques however have assessed the clinically realistic situation of considering both tumor and normal cells within the target volume. This study considers a ratio-based fluence optimizing technique to compare a dose-based optimization method described previously and two biologically based models. The biologically based methods use the values of equivalent uniform dose calculated for the tumor cells and integral biological effective dose for normal cells. The first biologically based method includes only tumor cells in the target volume while the second considers both tumor and normal cells in the target volume. All three methods achieve good conformation to the target volume. The biologically based optimization without the normal tissue in the target volume shows a high dose region in the center of the target volume while this is reduced when the normal tissues are also considered in the target volume. This effect occurs because the normal tissues in the target volume require the optimization to reduce the dose and therefore limit the maximum dose to that volume. © *2002 American Association of Physicists in Medicine.* [DOI: 10.1118/1.1487420]

Key words: radiobiological models, optimization, normal and tumor cells

TABLE I. The dose parameters resulting for the different algorithms for the dose distributions when the minimum dose is set to 40 Gy.

	Physical optimization (R_P)	Biological optimization 1 (R_{biol1})	Biological optimization 2 (R_{biol2})
Maximum tumor dose (Gy)	65	116	86
Minimum tumor dose (Gy)	40	40	40
Maximum critical dose (Gy)	40	52	46
Maximum normal dose (Gy)	54	68	76
EUD tumor (Gy_{10})	52	53	52
IBED critical (Gy_3)	36	27	31
IBED normal (Gy_3)	22	27	31

TABLE II. The dose parameters resulting for the different algorithms for the dose distributions when the tumor EUD is set to 60 Gy_{10}.

	Physical optimization (R_P)	Biological optimization 1 (R_{biol1})	Biological optimization2 (R_{biol2})
Maximum tumor dose (Gy)	78	137	104
Minimum tumor dose (Gy)	48	48	48
Maximum critical dose (Gy)	46	62	56
Maximum normal dose (Gy)	65	80	92
EUD tumor (Gy_{10})	60	60	60
IBED critical (Gy_3)	40	34	39
IBED normal (Gy_3)	26	29	36

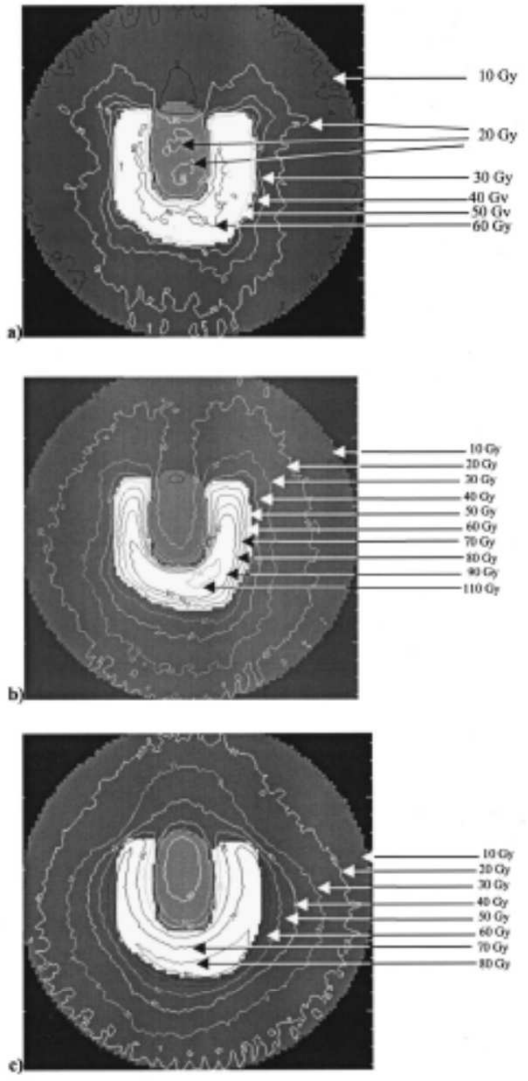

FIG. 2. Comparison between the resulting dose distributions for the different algorithms when the minimum physical dose is set to 40 Gy using (a) the physical optimization algorithm (R_P), (b) the biological optimization algorithm without normal tissues in the target volume (R_{biol1}), and (c) the biological optimization algorithm with normal tissues in the target volume (R_{biol2}).

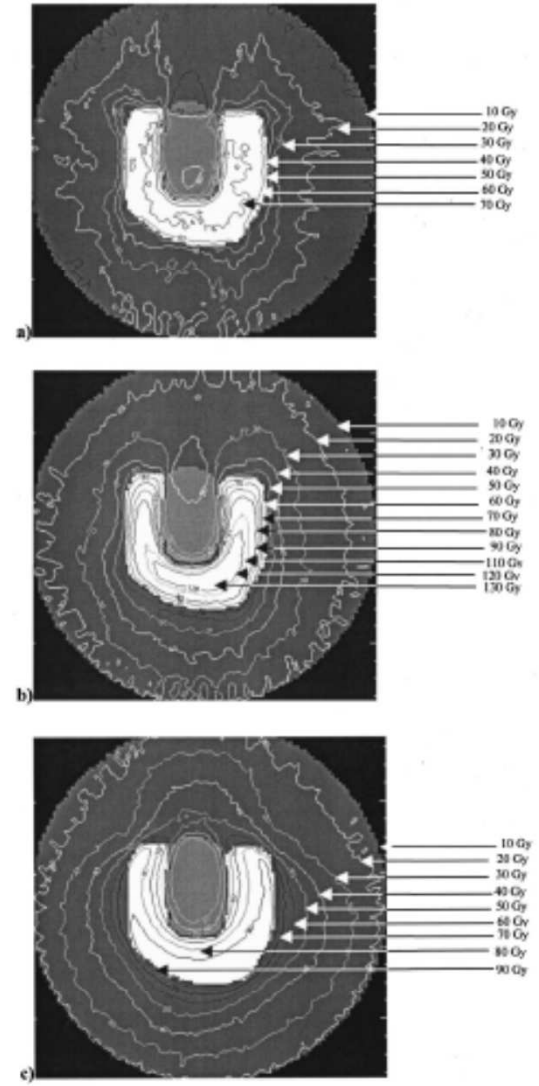

FIG. 3. Comparison between the resulting dose distributions for the different algorithms when the EUD to the tumor is set to 60 Gy_{10} using (a) the physical optimization algorithm (R_P), (b) the biological optimization algorithm without normal tissues in the target volume (R_{biol1}), and (c) the biological optimization algorithm with normal tissues in the target volume (R_{biol2}).

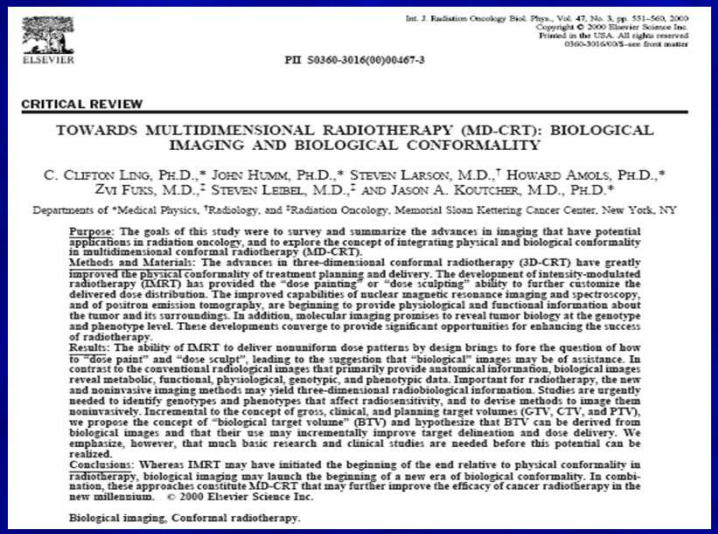

Int. J. Radiation Oncology Biol. Phys., Vol. 47, No. 3, pp. 551–560, 2000

0360-3016/00/$–see front matter

ELSEVIER

PII S0360-3016(00)00467-3

CRITICAL REVIEW

TOWARDS MULTIDIMENSIONAL RADIOTHERAPY (MD-CRT): BIOLOGICAL IMAGING AND BIOLOGICAL CONFORMALITY

C. Clifton Ling, Ph.D.,* John Humm, Ph.D.,* Steven Larson, M.D.,† Howard Amols, Ph.D.,* Zvi Fuks, M.D.,‡ Steven Leibel, M.D.,‡ and Jason A. Koutcher, M.D., Ph.D.*

Departments of *Medical Physics, †Radiology, and ‡Radiation Oncology, Memorial Sloan Kettering Cancer Center, New York, NY

Purpose: The goals of this study were to survey and summarize the advances in imaging that have potential applications in radiation oncology, and to explore the concept of integrating physical and biological conformality in multidimensional conformal radiotherapy (MD-CRT).

Methods and Materials: The advances in three-dimensional conformal radiotherapy (3D-CRT) have greatly improved the physical conformality of treatment planning and delivery. The development of intensity-modulated radiotherapy (IMRT) has provided the "dose painting" or "dose sculpting" ability to further customize the delivered dose distribution. The improved capabilities of nuclear magnetic resonance imaging and spectroscopy, and of positron emission tomography, are beginning to provide physiological and functional information about the tumor and its surroundings. In addition, molecular imaging promises to reveal tumor biology at the genotype and phenotype level. These developments converge to provide significant opportunities for enhancing the success of radiotherapy.

Results: The ability of IMRT to deliver nonuniform dose patterns by design brings to fore the question of how to "dose paint" and "dose sculpt", leading to the suggestion that "biological" images may be of assistance. In contrast to the conventional radiological images that primarily provide anatomical information, biological images reveal metabolic, functional, physiological, genotypic, and phenotypic data. Important for radiotherapy, the new and noninvasive imaging methods may yield three-dimensional radiobiological information. Studies are urgently needed to identify genotypes and phenotypes that affect radiosensitivity, and to devise methods to image them noninvasively. Incremental to the concept of gross, clinical, and planning target volumes (GTV, CTV, and PTV), we propose the concept of "biological target volume" (BTV) and hypothesize that BTV can be derived from biological images and that their use may incrementally improve target delineation and dose delivery. We emphasize, however, that much basic research and clinical studies are needed before this potential can be realized.

Conclusions: Whereas IMRT may have initiated the beginning of the end relative to physical conformality in radiotherapy, biological imaging may launch the beginning of a new era of biological conformality. In combination, these approaches constitute MD-CRT that may further improve the efficacy of cancer radiotherapy in the new millennium. © 2000 Elsevier Science Inc.

Biological imaging, Conformal radiotherapy.

Anatomical images

- X-ray
- Ultrasound
- CT
- MRI

Biological images

Metabolic
Biochemical
Physiological
Functional
Should also encompass molecular, genotypic and phenotypic images

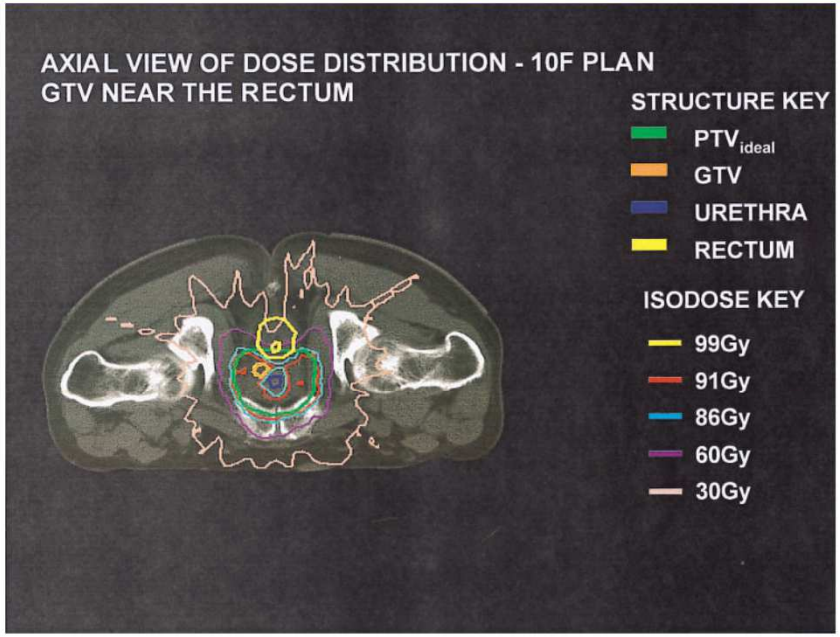

Fig. 1. An example of an ultraconformal, or "dose painted" external beam treatment of the prostate. We assume that biological imaging techniques exist which permit localization of regions within the prostate that contain highest tumor burden (GTV, outlined in orange), and also identification of urethra (blue outline) and prostatic capsule (PTV, green outline). This 10-field plan demonstrates the exquisite capability, using the existing MSKCC inverse treatment planning system, to sculpt the dose to the desired shape.

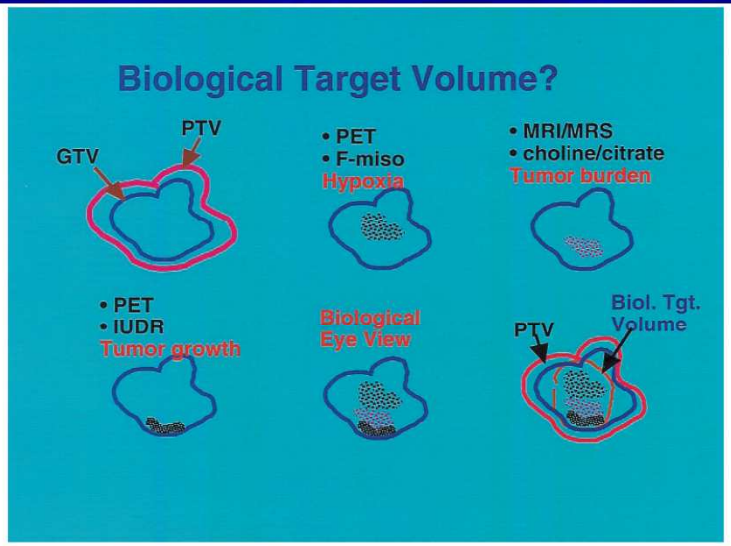

Fig. 2. An idealized schematic illustrating the concept of biological target volume (BTV). Whereas at present the target volume is characterized by the concepts of GTV, CTV, and PTV, biological images as depicted in Fig. 2 may provide information for defining the BTV to improve dose targeting to certain regions of the target volume. For example, regions of low pO_2 level may be derived from PET-^{18}F-misonidazole study, high tumor burden from MRI/MRS data of choline/citrate ratio, and high proliferation from PET-^{124}IUdR measurement.

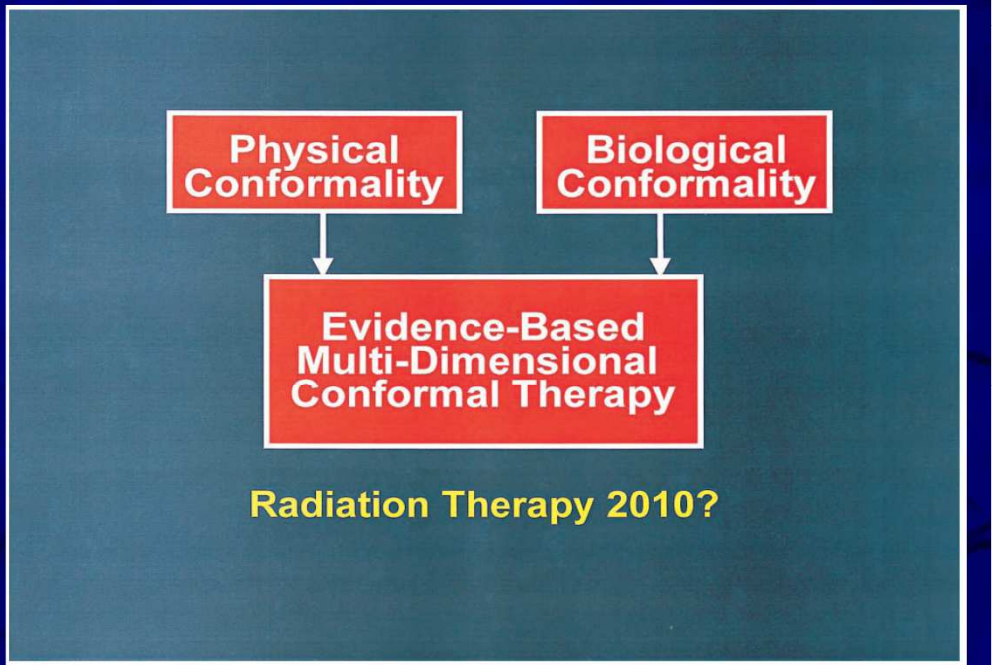

Fig. 3. MD-CRT combines the attributes of physical conformality of 3D-CRT, and the dose targeting ability of IMRT to conform the dose pattern to the radiobiological features of the target that may be derived from biological imaging.

INSTITUTE OF PHYSICS PUBLISHING PHYSICS IN MEDICINE AND BIOLOGY
Phys. Med. Biol. 47 (2002) 3567–3578 PII: S0031-9155(02)36593-X

Inverse planning for functional image-guided intensity-modulated radiation therapy

Lei Xing[1], Cristian Cotrutz[1], Sandeep Hunjan[1], Arthur L Boyer[1], Elfar Adalsteinsson[2] and Daniel Spielman[2]

[1] Department of Radiation Oncology, Stanford University School of Medicine, Stanford, CA 94305-5304, USA
[2] Department of Radiology and Lucas Center for Magnetic Resonance Image and Spectroscopy, Stanford University School of Medicine, Stanford, CA 94305-5488, USA

E-mail: lei@reyes.stanford.edu

Received 3 May 2002, in final form 13 August 2002
Published 3 October 2002
Online at stacks.iop.org/PMB/47/3567

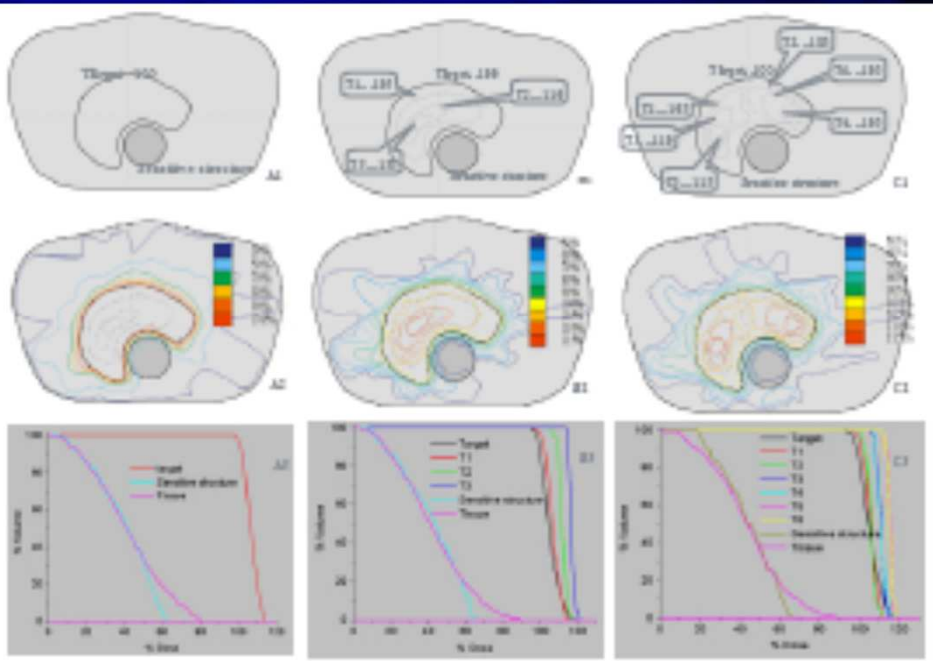

Figure 1. Flow chart of functional image-guided IMRT planning process.

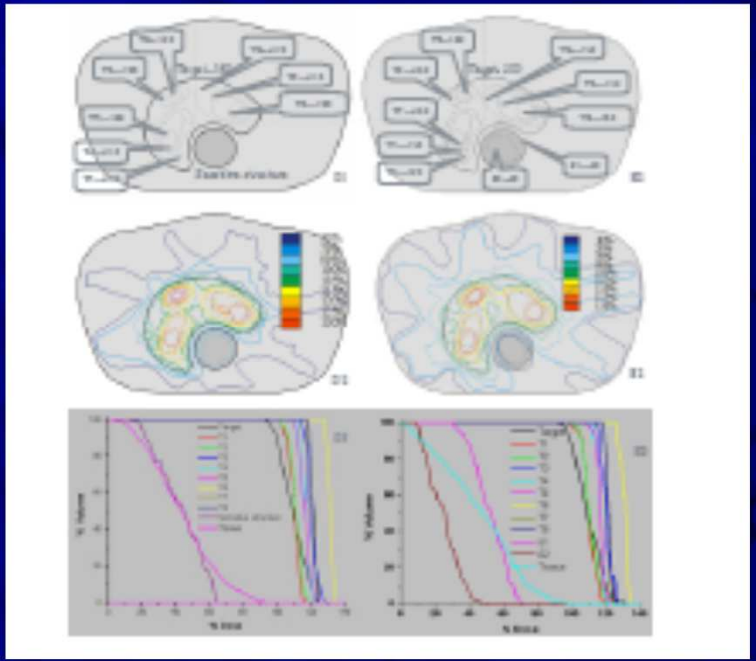

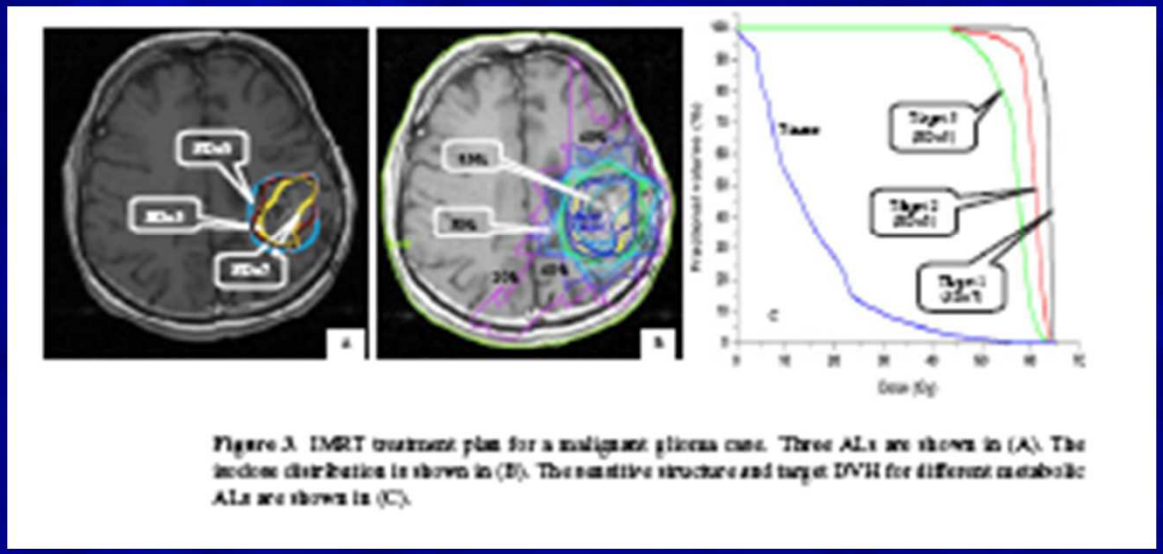

Figure 3. IMRT treatment plan for a malignant glioma case. Three ALs are shown in (A). The isodose distribution is shown in (B). The sensitive structure and target DVH for different metabolic ALs are shown in (C).

Radiobiologically based indices

Tumour control probability (TCP)
Normal tissue complication probability (NTCP)
Equivalent uniform dose distribution (EUD)
Biologically effective uniform dose (BUD)

Phys. Med. Biol. 48 (2003) N31–N35 PII: S0031-9155(03)38715-9

NOTE

On biologically conformal boost dose optimization

M Alber[1], F Paulsen[2], S M Eschmann[3] and H J Machulla[4]

[1] Department of Medical Physics, University of Tübingen, Tübingen, Germany
[2] Clinic for Radiation Oncology, University of Tübingen, Tübingen, Germany
[3] Department of Nuclear Medicine, University of Tübingen, Tübingen, Germany
[4] Department of Radiopharmacy, University of Tübingen, Tübingen, Germany

Received 26 June 2002
Published 8 January 2003
Online at stacks.iop.org/PMB/48/N31

Abstract
A method is described that allows the inclusion of biological imaging data in the optimization of intensity-modulated radiotherapy to produce dose boosts that conform with target subvolumes of potentially reduced radiosensitivity. The biological image (e.g. PET, fMRI, etc) is transformed into a dose efficiency distribution using a piecewise linear calibration function with a prescribed maximum boost factor. Instead of dose alone, the cost function of the optimization algorithm depends on the product of the physical dose times dose efficiency. An example case of a base-of-tongue tumour which was imaged with the hypoxia tracer fluoro-misonidazole is presented, showing the excellent capability of IMRT to produce dose distributions that conform to spatially variable dose prescriptions.

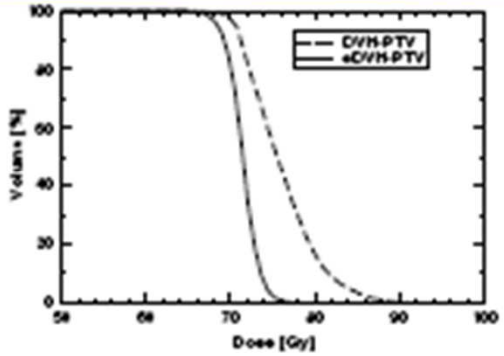

Figure 3. The cumulative dose–volume histogram of the target volume together with a histogram showing the effective dose as the product of dose efficiency and dose.

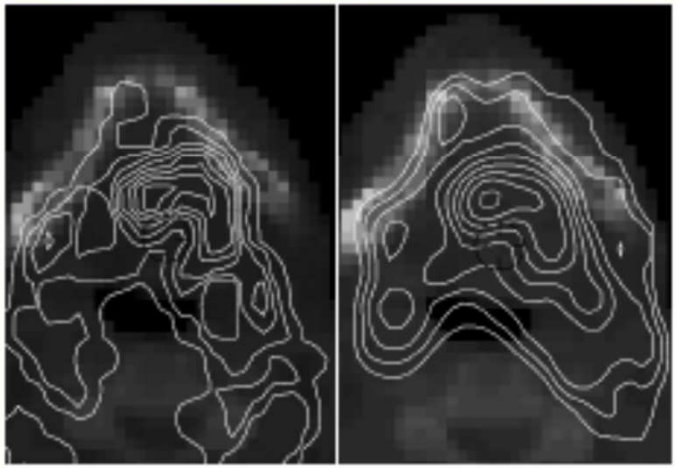

Figure 1. A transversal view of the dose-efficiency map as transformed from the PET image (left) and the dose distribution of a base of tongue tumour. The isolines correspond to, from outermost line to innermost: 99%, 96%, 93%, 90%, 87%, 84%, 81%, 78% dose efficiency levels. Right, the dose distribution with isolines of 95%, 100%, 104%, 108%, 112%, 116%, 120%, 124%, 128%. The isolines of the density image have been de-noised to enhance clarity.

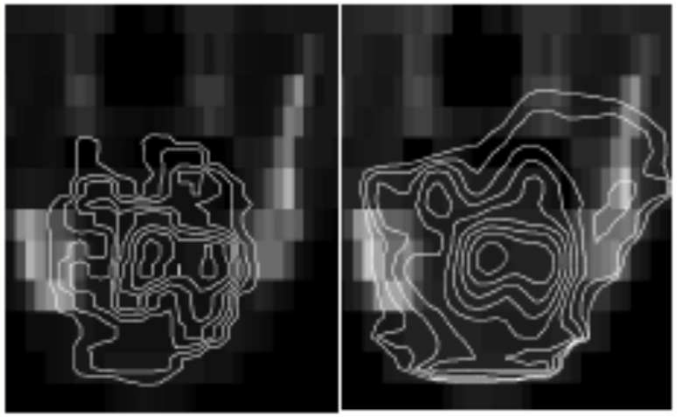

Figure 2. Coronal view of the dose-efficiency map (left) and the dose distribution. The isolines

Towards biologically conformal radiation therapy (BCRT): Selective IMRT dose escalation under the guidance of spatial biology distribution

Yong Yang and Lei Xing[a)]
Department of Radiation Oncology, Stanford University School of Medicine, Stanford, California 94305-5847

(Received 28 September 2004; revised 17 March 2005; published 11 May 2005)

It is well known that the spatial biology distribution (e.g., clonogen density, radiosensitivity, tumor proliferation rate, functional importance) in most tumors and sensitive structures is heterogeneous. Recent progress in biological imaging is making the mapping of this distribution increasingly possible. The purpose of this work is to establish a theoretical framework to quantitatively incorporate the spatial biology data into intensity modulated radiation therapy (IMRT) inverse planning. In order to implement this, we first derive a general formula for determining the desired dose to each tumor voxel for a known biology distribution of the tumor based on a linear-quadratic model. The desired target dose distribution is then used as the prescription for inverse planning. An objective function with the voxel-dependent prescription is constructed with incorporation of the nonuniform dose prescription. The functional unit density distribution in a sensitive structure is also considered phenomenologically when constructing the objective function. Two cases with different hypothetical biology distributions are used to illustrate the new inverse planning formalism. For comparison, treatments with a few uniform dose prescriptions and a simultaneous integrated boost are also planned. The biological indices, tumor control probability (TCP) and normal tissue complication probability (NTCP), are calculated for both types of plans and the superiority of the proposed technique over the conventional dose escalation scheme is demonstrated. Our calculations revealed that it is technically feasible to produce deliberately nonuniform dose distributions with consideration of biological information. Compared with the conventional dose escalation schemes, the new technique is capable of generating biologically conformal IMRT plans that significantly improve the TCP while reducing or keeping the NTCPs at their current levels. Biologically conformal radiation therapy (BCRT) incorporates patient-specific biological information and provides an outstanding opportunity for us to truly individualize radiation treatment. The proposed formalism lays a technical foundation for BCRT and allows us to maximally exploit the technical capacity of IMRT to more intelligently escalate the radiation dose. © *2005 American Association of Physicists in Medicine*. [DOI: 10.1118/1.1924312]

Key words: inverse planning, biological model, TCP, NTCP, IMRT

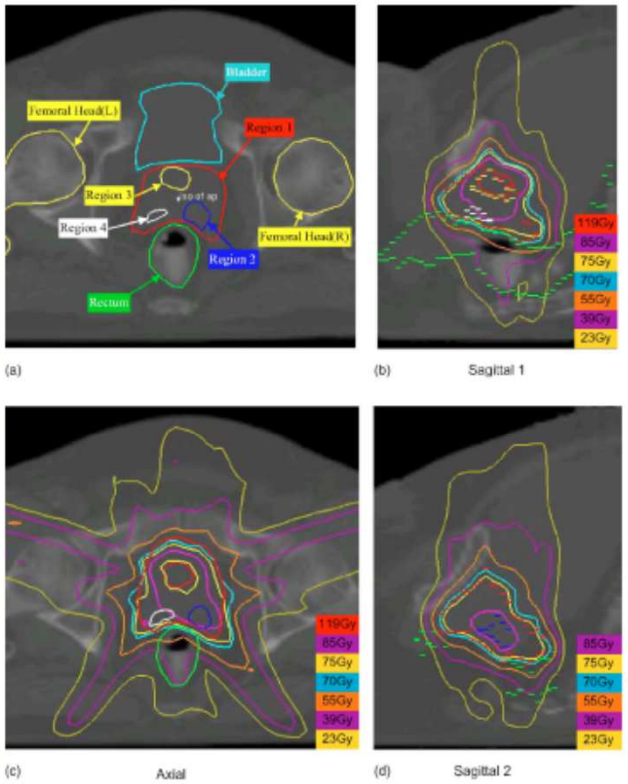

FIG. 1. A hypothetical prostate case with four biologically different regions (example 1). (a) Geometric shapes and locations of the targets and sensitive structures; (b)–(d): Isodose distributions in an axial slice and two sagittal slices for plan 1, generated by optimizing the objective function with a nonuniform dose prescription derived from Eq. (7).

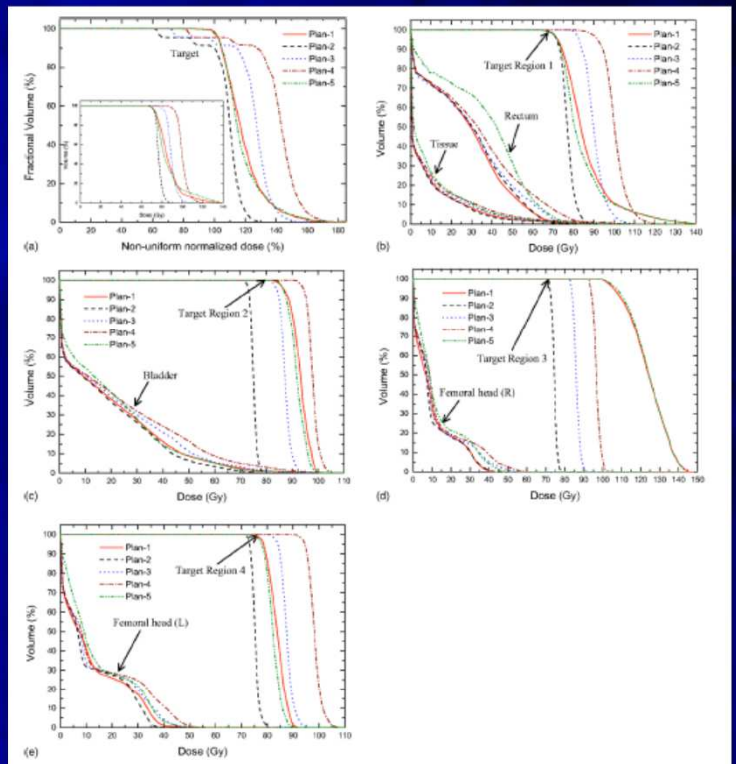

FIG. 2. Comparison of EDVHs and DVHs of the BCRT plan (plan 1), three uniform IMRT plans (plan 2: 70 Gy, plan 3: 81 Gy, and plan 4: 91 Gy) and the SIB plan (plan 5) in example 1. (a) Target EDVHs for the five plans (inset is the regular DVHs of the prostate target). The normalized doses to the target region 1, 2, 3 and 4 are 70, 85, 119, and 75 Gy, respectively; (b)-(e) DVHs of different target regions and sensitive structures for the five plans. The solid, dashed, dotted, dash-dotted, and dash-dot-dotted curves represent the results of plan 1, 2, 3, 4, and 5, respectively. The effective dose is defined as the physical dose at a voxel normalized by its desired dose determined by Eq. (7).

TABLE III. Comparison of TCP and NTCP for the five IMRT plans for example 1.

		Plan 1 (BCRT plan)	Plan 2 (70 Gy Uniform)	Plan 3 (81 Gy Uniform)	Plan 4 (91 Gy Uniform)	Plan 5 (SIB plan)
TCP	Region 1	0.997	0.995	1.000	1.000	0.994
	Region 2	0.998	0.642	0.995	1.000	0.999
	Region 3	0.989	0.000	0.002	0.461	0.989
	Region 4	1.000	0.997	1.000	1.000	0.998
	Overall	0.984	0.000	0.002	0.461	0.981
NTCP (%)	Rectum	0.212	0.196	0.652	1.84	0.885
	Bladder	1.6×10^{-5}	1.4×10^{-5}	2.3×10^{-5}	4.2×10^{-5}	3.6×10^{-5}
	Femoral head (R)	2.0×10^{-5}	2.1×10^{-6}	2.6×10^{-4}	1.75×10^{-4}	3.9×10^{-5}
	Femoral head (L)	1.2×10^{-5}	2.0×10^{-6}	7.0×10^{-4}	5.26×10^{-4}	6.9×10^{-5}

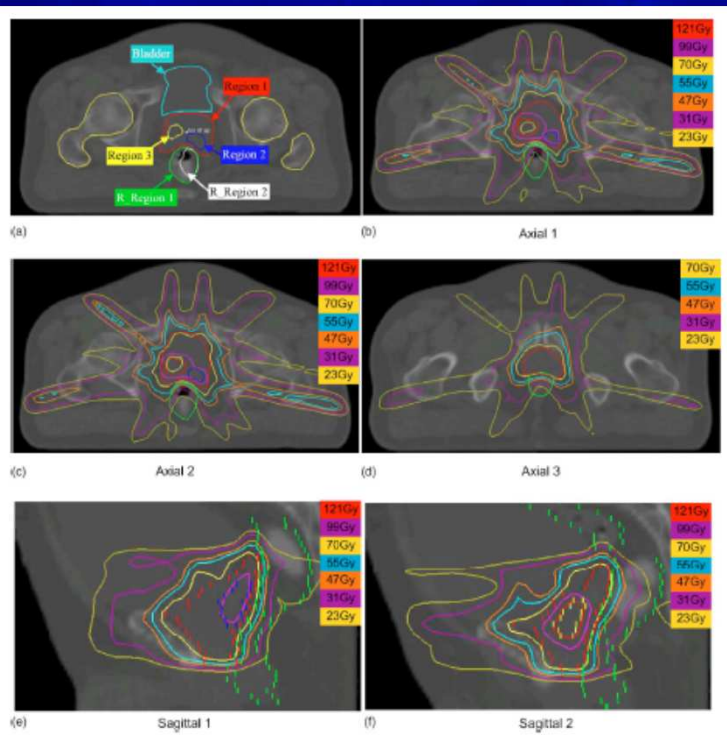

FIG. 3. A hypothetical prostate case with three biologically different regions and nonuniform importance in the rectum (example 2). (a) Geometric shapes and locations of the targets and sensitive structures; (b)–(d) Isodose distributions in three axial slices and two sagittal slices for plan 1, generated by optimizing the objective function with nonuniform dose prescription derived from Eq. (7).

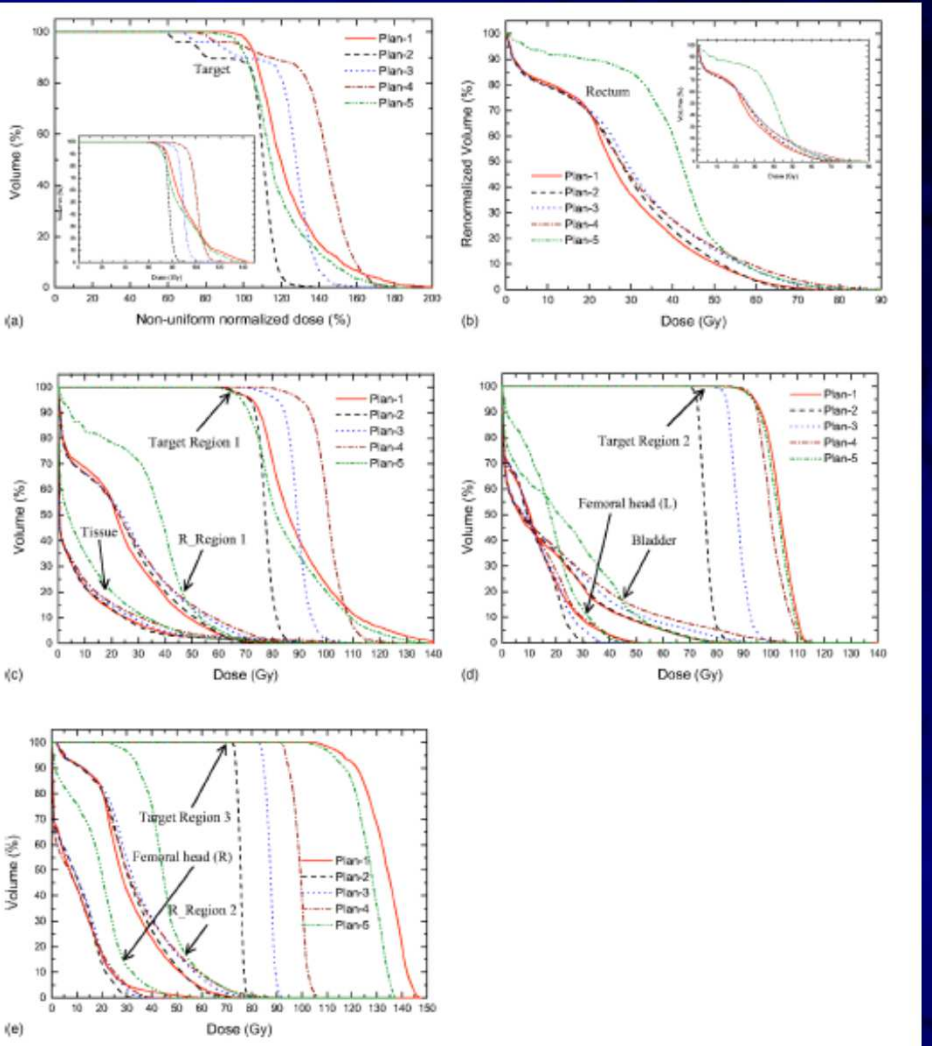

FIG. 4. Comparison of EDVHs, FDVHs, and DVHs of the BCRT plan (plan 1), three uniform IMRT plans (plan 2: 70 Gy, plan 3: 81 Gy, and plan 4: 91 Gy) and the SIB plan (plan 5) in example 2. (a) The target EDVHs for the five plans (insert is the regular DVHs of the prostate target). The normalized doses to the target region 1, 2, and 3 are 70, 99, and 121 Gy, respectively; (b) The rectum FDVHs for the five plans (insert is the regular DVHs of the rectum); (c)–(e): DVHs of different target regions and sensitive structures for the five plans. The solid, dashed, dotted, dash-dotted, and dash-dot-dotted curves represent the results of plan 1, 2, 3, 4, and 5, respectively.

TABLE IV. Comparison of TCP and NTCP for the five IMRT plans for example 2.

		Plan 1 (BCRT plan)	Plan 2 (70 Gy Uniform)	Plan 3 (81 Gy Uniform)	Plan 4 (91 Gy Uniform)	Plan 5 (SIB Plan)
TCP	Region 1	0.997	0.995	1.000	1.000	0.968
	Region 2	0.989	0.000	0.587	0.981	0.987
	Region 3	0.996	0.006	0.408	0.839	0.990
	Overall	0.981	0.000	0.239	0.823	0.946
NTCP (%)	Rectum	0.397	0.414	1.46	3.12	1.25
	Bladder	1.5×10^{-5}	1.2×10^{-5}	1.8×10^{-5}	4.3×10^{-5}	3.9×10^{-5}
	Femoral head (R)	3.7×10^{-5}	1.5×10^{-5}	1.8×10^{-5}	5.3×10^{-5}	2.3×10^{-5}
	Femoral head (L)	4.9×10^{-5}	1.1×10^{-5}	3.0×10^{-5}	4.5×10^{-5}	3.6×10^{-5}

BGRT: Biologically guided radiation therapy—The future is fast approaching!

Robert D. Stewart
School of Health Sciences, Purdue University, 550 Stadium Mall Drive, West Lafayette, Indiana 47907-2051

X. Allen Li[a)]
Department of Radiation Oncology, Medical College of Wisconsin, 8701 Watertown Plank Road, Milwaukee, Wisconsin 53226

(Received 3 January 2007; revised 9 August 2007; accepted for publication 10 August 2007; published 11 September 2007)

Rapid advances in functional and biological imaging, predictive assays, and our understanding of the molecular and cellular responses underpinning treatment outcomes herald the coming of the long-sought goal of implementing patient-specific biologically guided radiation therapy (BGRT) in the clinic. Biological imaging and predictive assays have the potential to provide patient-specific, three-dimensional information to characterize the radiation response characteristics of tumor and normal structures. Within the next decade, it will be possible to combine such information with advanced delivery technologies to design and deliver biologically conformed, individualized therapies in the clinic. The full implementation of BGRT in the clinic will require new technologies and additional research. However, even the partial implementation of BGRT treatment planning may have the potential to substantially impact clinical outcomes. [DOI: 10.1118/1.2779861]

Key words: biologically guided radiation therapy, biological imaging, outcome modeling, LQ model

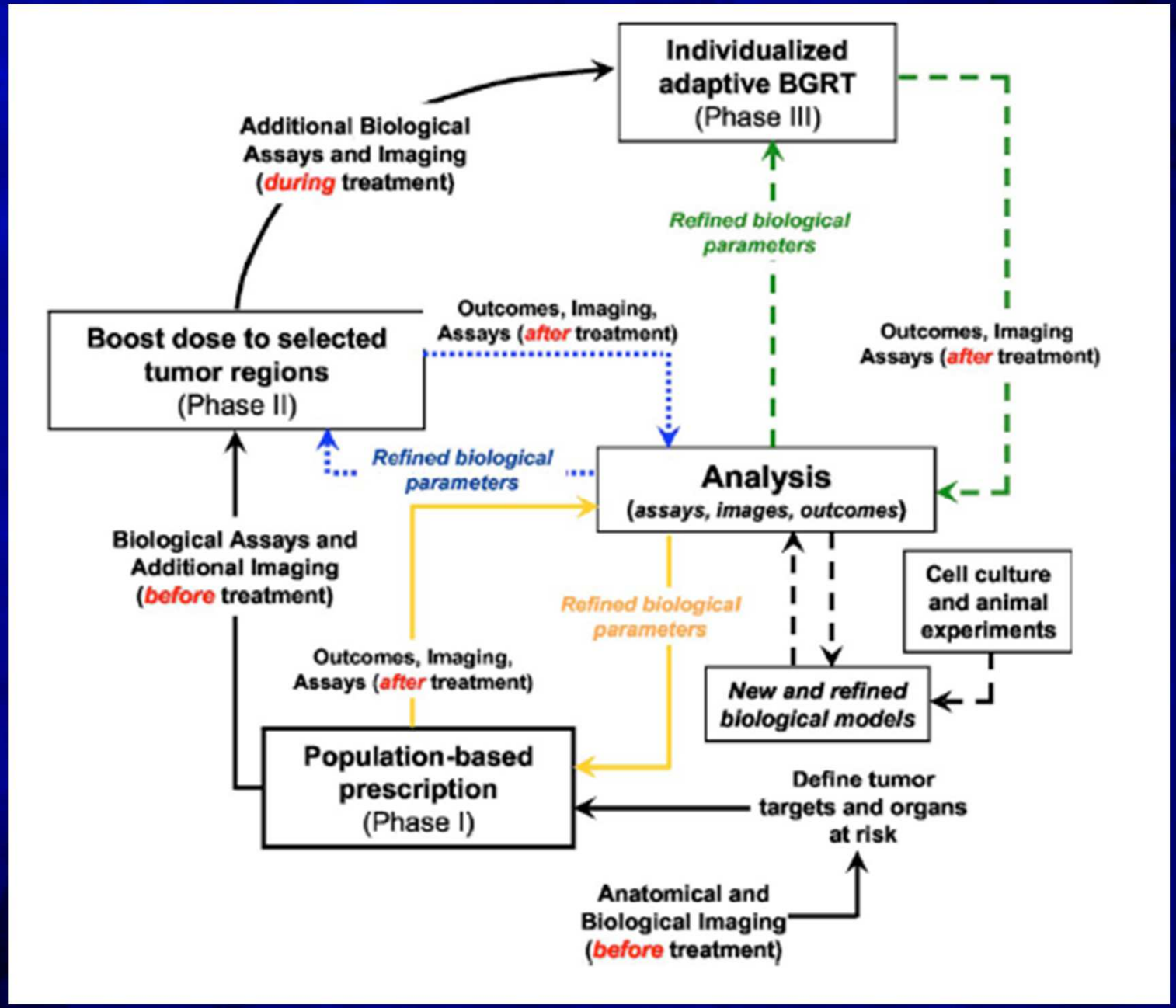
Individualized adaptive BGRT (Phase III)
Additional Biological Assays and Imaging (during treatment)
Refined biological parameters
Boost dose to selected tumor regions (Phase II)
Outcomes, Imaging, Assays (after treatment)
Outcomes, Imaging Assays (after treatment)
Refined biological parameters
Analysis (assays, images, outcomes)
Biological Assays and Additional Imaging (before treatment)
Refined biological parameters
Cell culture and animal experiments
Outcomes, Imaging, Assays (after treatment)
New and refined biological models
Population-based prescription (Phase I)
Define tumor targets and organs at risk
Anatomical and Biological Imaging (before treatment)

The more I know,
the less I understand
All the things I thought I knew,
I have to learn again

Happiness Is

- At age 4 … not peeing in your pants
- At age 12 … having friends
- At age 16 … having a driver's license
- At age 25… having sex when married
- At age 35 … having money
- At age 50 … having money
- At age 60 … having sex when married
- At age 70 … having a driver's license
- At age 75 … having friends
- At age 80 … not peeing in your pants

Thanks for
Downloading

Thanks and keep smiling